Synthesis and Self-Assembly of [60]Fullerene Containing Sulfobetaine Polymer in Aqueous Solution

P. Ravi, S. Dai,† and K. C. Tam*

Singapore-MIT Alliance and School of Mechanical and Aerospace Engineering, Nanyang Technological University, 50 Nanyang Avenue, Singapore 639798, Republic of Singapore

Received: June 9, 2005; In Final Form: September 22, 2005

A well-defined poly(2-(dimethylamino)ethyl methacrylate) (PDMAEMA-*b*-C_{60}) was synthesized using the atom transfer radical polymerization (ATRP) technique and betainized with 1,3-sulfobetaine to yield a Bet-PDMAEMA-*b*-C_{60}. The solution properties were then studied by light transmittance, viscometric, ^{1}H NMR laser light scattering, and transmission electron macroscopic techniques. It was found that Bet-PDMAEMA-*b*-C_{60} exhibits an upper critical solution temperature (USCT) similar to that observed for Bet-PDMAEMA in aqueous solution. However, the modification of Bet-PDMAEMA with a C_{60} molecule increases the UCST of Bet-PDMAEMA in solution, which is a function of the solution ionic strength. Addition of a small amount of salt increases the UCST, similar to polyelectrolyte systems, while the presence of an excess amount of salt leads to a decrease in the UCST, attributed to the antipolyelectrolyte effect of polyampholytes. In aqueous salt solution, Bet-PDMAEMA-*b*-C_{60} chains self-assemble into micelles that coexist with unimeric Bet-PDMAEMA-*b*-C_{60} chains. TEM studies revealed that the system agglomerates when the temperature exceeds the UCST.

Introduction

[60]Fullerene (C_{60}) exhibits unique properties, such as electronic,[1] conducting,[2] magnetic, and high cohesive forces between C_{60} molecules,[3] the ability to accept and release electrons,[4] and relatively high reactivity that allows tailoring of C_{60}-based derivatives,[5,6] which hold promising end-use applications.[7,8] However, the complete lack of solubility of C_{60} molecules in most organic solvents and aqueous solution hampers its processability and potential applications. Several methods have been adopted to increase its solubility, for example, by forming complexes with surfactants or cyclodextrins through solubilization and encapsulation,[9,10] producing a charge-transfer (CT) complex with organic compounds bearing electron-donating groups through electron-donor and -acceptor interaction,[11] and conjugating functional groups such as carboxylic acids,[12] amines,[13] or alcohols[14] onto C_{60} molecules. Grafting long chain polymers onto C_{60} not only improves its solubility, but also retains the unique properties of pristine C_{60}, which is more amenable for further research.[15] By grafting well-defined hydrophilic polymers to fullerene molecules, C_{60}-containing water-soluble polymeric systems are obtained, and they could form different nanoscale aggregates with interesting morphologies due to their amphiphilic character.[16] Therefore, synthesizing novel materials by combining the unique properties of C_{60} and specific properties of polymer not only enhances its processability but also extends the desired end-use applications.[17]

The development of aggregates with different morphologies and the study on their aggregation mechanism in solution using well-defined polymeric system are of potential interest to the research community.[18] Self-assembled, C_{60}-containing polymers possess promising end-use applications.[19,20] Though several studies have been reported on the self-assembly behavior of fullerene-containing polymers in organic solvents,[16,21] there is a scarcity of reports describing the self-assembly behavior of well-defined fullerene-containing polymers in aqueous solution. Yang and co-workers reported the synthesis and aggregation behavior of poly(acrylic acid)-*b*-C_{60} (PAA-*b*-C_{60}) in aqueous solution, which forms a core−shell structure, whose microstructure controls the photoconductive properties.[22] Over the last couple of years, we have focused on the synthesis and self-assembly behavior of well-defined fullerene-containing polymers, especially the well-defined stimuli-responsive C_{60}-containing polyelectrolytes such as poly(2-(dimethylamino)ethyl methacrylate) (PDMAEMA-*b*-C_{60})[23] and poly(methacrylic acid)-*b*-C_{60} (PMAA-*b*-C_{60})[24,25] and polyampholytes such as PMAA-*b*-PDMAEMA-*b*-C_{60},[26] and their self-assembly behavior as a function of pH and temperature. Both PDMAEMA-*b*-C_{60} and PMAA-*b*-C_{60} possess micellar-like aggregates at low and high pH, respectively. We have also demonstrated the use of negatively charged aggregates of PMAA-*b*-C_{60} or PAA-*b*-C_{60} to induce and control the formation of fractal patterns from nano- to microscopic scales.[25]

The first example of a synthetic polybetaine was reported by Ladenheim and Morawetz in 1957,[27] and an excellent review on this topic has recently been published by Lowe and McCormick.[28] Much interest has also been focused on the self-assembled structure of polyzwitterionic block polymers in aqueous solutions, due to their unique antipolyelectrolyte effect, i.e., chain expansion upon the addition of electrolyte (salt).[28] The most interesting property of polyzwitterionic polymers is that they can be used to mimic naturally occurring ampholytic polymers, such as protein near the isoelectric point (IEP) or DNA at low pH.[29] Their characteristics may respond to external stimuli such as temperature or ionic strength of the solution.[30] In aqueous solution, these polymers self-organize into different

* Corresponding author. Fax: (65) 6795 1859. E-mail: mkctam@ntu.edu.sg.

† Currently at the Department of Chemical Engineering, McMaster University, Hamilton, Ontario, L8S 4L7, Canada.

10.1021/jp053088h CCC: $30.25
Published on Web 11/12/2005

kinds of structures, depending on the hydrophobicity of the backbone and solvent quality. At low temperatures, their solutions are cloudy due to the strong intermolecular electrostatic attractive interaction. When the temperature exceeds the upper critical solution temperature (UCST), where the thermal energy is larger than the electrostatic attraction, the solution becomes clear.[31]

Different kinds of polyzwitterionic polymers and their copolymers have been developed, and their aqueous solution properties were studied.[32−36] Armes and co-workers studied the salt dependency on the chain expansion of micellar aggregates produced from betainized PDMAEMA-*b*-PMMA.[37] However, a detailed study on the dependence of UCST on salt concentration has not been reported. In addition, there is no reported study on the self-assembly behavior of well-defined C_{60}-containing polyzwitterionic polymers. For C_{60}-containing polyzwitterionic polymer, the chemical structure, molecular weight, polymer concentration, ionic strength, and temperature play important roles in controlling the self-assembly behavior of the system. Because of the potential applications of both C_{60} and polyzwitterionic polymers in biological science,[38,39] we synthesized such a well-defined mono-end-capped C_{60} with polysulfobetaine polymer and studied its self-assembly behavior as a function of temperature and salt concentration.

Experimental Section

Materials. C_{60} (>99.5%) and 2-(dimethylamino)ethyl methacrylate (DMAEMA, 98%) monomer were purchased from MTR Ltd and Sigma-Aldrich, respectively. 1,1,4,7,10,10-Hexamethyltriethylenetetramine (HMTETA, 97%, Aldrich), CuCl (99.99%, Aldrich), and *p*-toluenesulfonyl chloride (99%, Fluka) were used as received. DMAEMA was passed through a basic alumina column, dried overnight over CaH_2, and then distilled under reduced pressure. All the solvents used in the synthesis were freshly distilled. For polymer solution preparation, deionized water used was from a Millipore Alpha-Q purification system equipped with a 0.22 μm filter, while HCl, NaOH, and NaCl (Merck) were used to adjust pH and ionic strength.

Synthesis of Betainized PDMAEMA-*b*-C_{60} Polymer. The synthesis and characterization details of well-defined mono-end-capped C_{60}-containing PDMAEMA polymer (PDMAEMA-*b*-C_{60}) were reported previously.[23] The M_n of the PDMAEMA-*b*-C_{60} determined from GPC (with respect to polystyrene standards) was 13 000 Da (M_n determined from ^{1}H NMR is 13 500 Da) with a polydispersity index (PDI) of 1.18. For the synthesis of betainized PDMAEMA-*b*-C_{60} polymer (Bet-PDMAEMA-*b*-C_{60}), about 4 g of PDMAEMA-*b*-C_{60} was solubilized in 60 mL of THF in a 100-mL round-bottom flask equipped with a magnetic stirring bar. 1,3-Propane sultone (2 equiv to DMAEMA monomer segments) was added to the reaction mixture and the solution was stirred at room temperature for 16 h. During betainization, the polymer became a gel and precipitated from solution. After the completion of the betainization reaction, THF was completely removed in a rotary evaporator and the final polymer was dried at room temperature under vacuum. An excess amount of 1,3-propane sultone was removed by Soxhlet extraction using THF to yield a brown-colored betainized PDMAEMA-*b*-C_{60}.

Ultraviolet−Visible Spectroscopy (UV). A HP8453 UV−visible spectrophotometer equipped with a HP89090A temperature control unit was used to measure the absorption and transmittance of the polymer solutions at different temperatures and pHs. For the absorption study, the wavelength was scanned from 200 to 900 nm, while the wavelength was set to 600 nm for the transmittance experiments.

Viscometry. The efflux times of dilute Bet-PDMAEMA and Bet-PDMAEMA-*b*-C_{60} aqueous solutions in different concentrations of NaCl were measured at 25 °C using a Cannon PolyVISC automatic capillary viscometer. The temperature is controlled by an airbath consisting of an outer insulated chamber enclosed by a second inner chamber, where the viscometer and sample are continuously bathed in a thermally stabilized stream of air. The temperature is controlled to within 0.01 °C with advanced measuring electronics, thermoelectric cooling, and controlling software. The measured efflux times were then converted to the relative viscosity using the following relationship

$$\eta_r = \frac{t}{t_0} \tag{1}$$

where t and t_0 are the efflux times for similar concentration of Bet-PDMAEMA or Bet-PDMAEMA-*b*-C_{60} in salt solution and in water, respectively.

NMR Spectroscopy. The ^{1}H NMR spectrum of the Bet-PDMAEMA-*b*-C_{60} was measured using a Brüker DRX400 instrument in D_2O at different temperatures.

Laser Light Scattering. A Brookhaven BI-200SM goniometer system equipped with a 532-channel BI9000AT digital multiple τ correlator was used to perform laser light scattering experiments. For static light scattering (SLS), a Berry-plot was used to analyze the experimental data, and the refractive index increment was measured using a BIDNDC differential refractometer. For dynamic light scattering (DLS), the inverse Laplace transform of REPES in the Gendist software package was used to analyze time correlation functions with the probability of reject set at 0.5. A 0.2 μm filter was used to remove dust prior to light scattering experiments, and the experimental temperature was controlled by a PolyScience water bath.

Transmission Electron Microscopy (TEM). Transmission electron microscopic studies were conducted using a JEOL JEM-2010 transmission electron microscope operating at an accelerate voltage of 200 kV. The carbon precoated copper grid was placed on a filter paper. For the TEM samples in the absence of salt (above UCST), a 0.2 wt % polymer solution was heated to 40 °C and a drop of solution was placed on a copper grid that was thermostated at 40 °C in an oven. For the TEM sample in the presence of salt, a drop of Bet-PDMAEMA-*b*-C_{60} in 0.5 M NaCl solution was placed on a copper grid and allowed to dry overnight at room temperature.

Results and Discussion

The synthesis and characterization of the well-defined PDMAEMA-*b*-C_{60} has been reported previously.[23] The typical synthesis route for Bet-PDMAEMA-*b*-C_{60} is shown in Scheme 1. Since the DMAEMA segment is highly reactive toward quaternization, selective betainization of PDMAEMA was achieved at ambient temperature using 1,3-propane sultone in THF.[37] After complete betainization, gelation occurs at room temperature, since the product is not soluble in THF. It has been demonstrated that under mild condition of betainization, chain scission did not occur. Hence, the narrow polydispersity of the polymer is retained in the resulting Bet-PDMAEMA-*b*-C_{60} system. The extent of betainization was calculated using a ^{1}H NMR spectrum (Figure 1) measured in the presence of 0.5 M NaCl in D_2O. From the relative peak intensities at 3.31 ppm [corresponds to the $-N(CH_3)_2$ protons of DMAEMA segments] and at 3.05 ppm (corresponds to $-CH_2SO_3^-$ protons of 1,3-

SCHEME 1: Synthesis Scheme of Bet-PDMAEMA-*b*-C_{60}

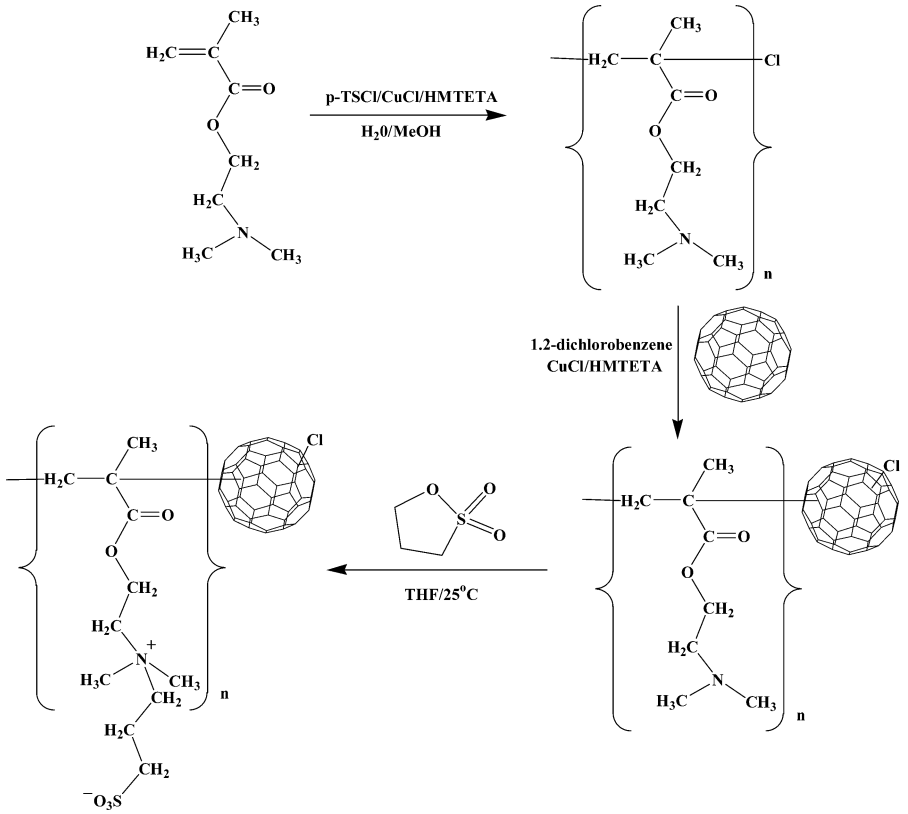

propane sultone segments), the extent of betainization was calculated to be more than 96%. The betainized polymer reported is the first example of monosubstituted well-defined C_{60}-containing sulfopropylbetine polymer (Bet-PDMAEMA-*b*-C_{60}).

Temperature Dependence of Solubility. At room temperature, Bet-PDMAEMA-*b*-C_{60} was water-insoluble due to the strong electrostatic attractive force from oppositely charged ion pairs along the polymer chains. When the temperature was increased to a critical value where the thermal energy is sufficient to overcome the electrostatic attractive force, Bet-PDMAEMA-*b*-C_{60} becomes water-soluble at a temperature that is referred to as the UCST. The solubility of both Bet-PDMAEMA-*b*-C_{60} and Bet-PDMAEMA as a function of temperature was examined and compared by light transmittance study using a UV−visible spectrophotometer at a fixed wavelength of 600 nm, and the UCST was determined from the first-order differential curve. Figure 2 compares the light transmittances of 0.1 wt % Bet-PDMAEMA-*b*-C_{60} and Bet-PDMAEMA in water over a temperature range from 20 to 50 °C. From the figure, it was evident that aqueous Bet-PDMAEMA solution is transparent over the experimental temperature range, indicating that its UCST is lower than 20 °C, which agrees with the reported UCST of less than 15 °C.[31] However, Bet-PDMAEMA-*b*-C_{60} exhibits a much higher UCST, thus it is water-insoluble at room temperature. With increasing temperature, the yellowish turbid solution becomes a translucent yellowish solution and the UCST of Bet-PDMAEMA-*b*-C_{60} in water was determined to be ∼32 °C. Attachment of a hydrophobic moiety to Bet-PDMAEMA alters the phase behavior to yield a higher UCST. However, the transition of Bet-PDMAEMA-*b*-C_{60} was found to be broad when compared to the lower critical solution temperature (LCST) of PDMAEMA-*b*-C_{60}, where the transition

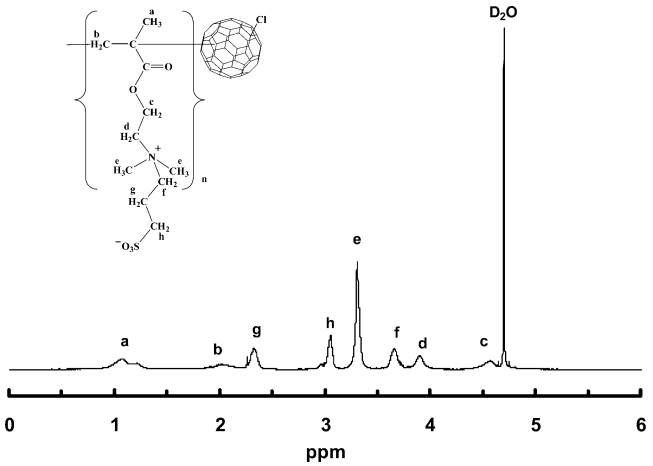

Figure 1. ^{1}H NMR spectrum of Bet-PDMAEMA-*b*-C_{60} in D_2O in the presence of 0.5 M NaCl.

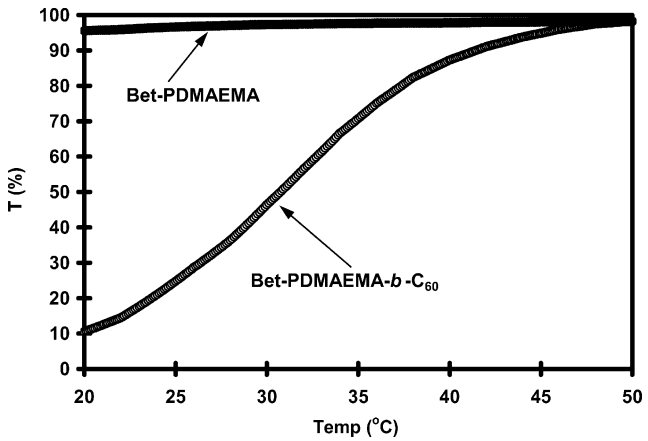

Figure 2. Light transmittance of Bet-PDMAEMA and Bet-PDMAEMA-*b*-C_{60} in aqueous solution at different temperatures.

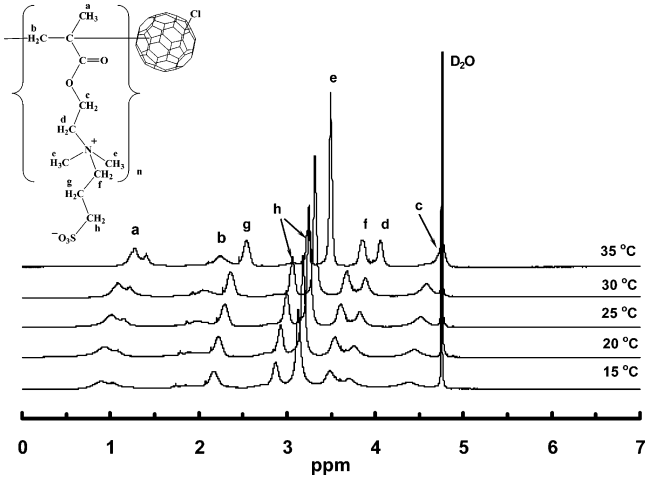

Figure 3. ^{1}H NMR spectra of Bet-PDMAEMA-*b*-C_{60} in D_2O measured at different temperatures.

is very sharp.[23] Generally, the transition for UCST is broader than for LCST, as the former is driven by an enthalpic effect, such as the disruption of solute−solute electrostatic interaction, while the later is controlled by an entropic effect, such as the disruption of H-bonds and water structures.

The phase behavior of Bet-PDMAEMA-*b*-C_{60} and the UCST was further confirmed by conducting ^{1}H NMR spectroscopic studies at different temperatures. Figure 3 shows the ^{1}H NMR spectrum of Bet-PDMAEMA-*b*-C_{60} in D_2O solution measured at different temperatures. At 20 °C, all the peaks corresponding to Bet-PDMAEMA segments, such as the signals at 0.85−1.1 ppm (backbone $-CH_3$), 2.14 ppm ($-CH_2CH_2SO_3^-$), 2.85 ppm ($-CH_2SO_3^-$), 3.66 ppm ($-COOCH_2CH_2N^+-$), 3.44 ppm ($-N^+CH_2CH_2CH_2-$), and 4.33 ppm ($-COOCH_2-$), were less pronounced. This indicates that large fractions of Bet-PDMAEMA segments are in the desolvated or collapsed state (less mobile) due to the strong intermolecular electrostatic attraction. However, small amounts of Bet-PDMAEMA segments are exposed in water as a solvated layer around the compact Bet-PDMAEMA surface, which can be observed from the ^{1}H NMR spectra. When the solution temperature was increased at an interval of 5 °C, the magnitude of the peaks corresponding to Bet-PDMAEMA segments is increased, corresponding to increasing proportions of mobile and solvated Bet-DMAEMA segments. At a temperature beyond the UCST (35 °C), where the thermal energy is sufficiently high in overcoming the electrostatic attraction, Bet-PDMAEMA-*b*-C_{60} becomes water-soluble. All the signals corresponding to Bet-PDMAEMA segments in the ^{1}H NMR spectra showed a pronounced maximum, and they shifted toward a lower field, confirming that the Bet-PDMAEMA segments are completely solvated (mobile).

Phase Behavior in the Presence of Salt. Due to the zwitterionic property of Bet-PDMAEMA-*b*-C_{60}, the presence of salt will alter the phase behavior of the polymer in aqueous solution. Figure 4 shows the UCST of Bet-PDMAEMA-*b*-C_{60} in aqueous solution as a function of NaCl concentration. The UCST of Bet-PDMAEMA-*b*-C_{60} increases initially in the low salt concentration regime. In absence of salt, the UCST of the polymer was determined to be 32 °C, it increases to a maximum of 49 °C at 0.35 wt % NaCl, and then it decreases again with increasing salt concentration. The observation is supported by viscometric and light transmittance studies. The inset in Figure 4 shows the NaCl concentration dependence of the relative viscosity of 0.3 wt % Bet-PDMAEMA-*b*-C_{60} and Bet-PDMAEMA at 25 °C, respectively. During the sample preparation,

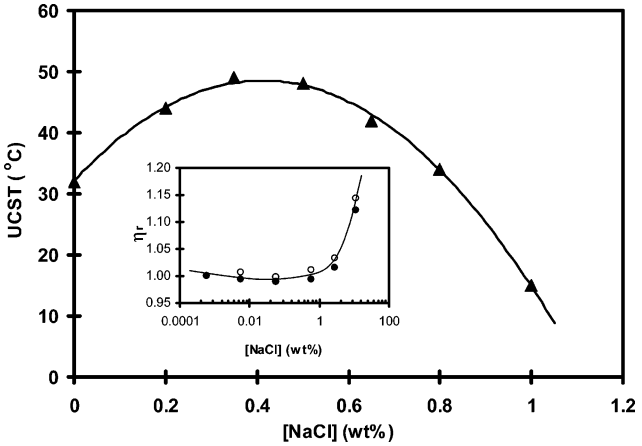

Figure 4. The effect of salt on the UCST of Bet-PDMAEMA-*b*-C_{60}. The inset shows the NaCl concentration dependence of the relative viscosity of 0.3 wt % Bet-PDMAEMA-*b*-C_{60} (filled circle) and Bet-PDMAEMA (open circle), respectively.

it is evident that the solution is very cloudy in the presence of 0.05 wt % of NaCl, which indicates the negative value of A_2. At a NaCl concentration less than 0.05 wt %, the relative viscosity of the solution decreases slightly or is unchanged, which indicates that the addition of salt could shield the electrostatic interaction, but the effect is not significant. However, with a further increase in the salt concentration, both the relative viscosity and solubility are enhanced. The increase in the reduced viscosity and A_2 values with increasing salt concentrations has been reported for other ampholytical polymers.[40] For Bet-PDMAEMA-*b*-C_{60} in solution at temperatures below the UCST, the intermolecular electrostatic attraction between oppositely charged ion pairs produces a compact chain conformation, which renders the polymer insoluble in aqueous solution. However, there are small amounts of ion pairs exposed to bulk water due to its zwitterionic property (Figure 5). The small amounts of added salt could bind to these exposed ion pairs. As a result, the polymer chains shrink, which not only facilitates an increasing proportion of intermolecular electrostatic interaction but also decreases the solubility of zwitterionic polymers in water. Since the UCST is related to the thermal energy required in overcoming the electrostatic attraction, the UCST of the polymer in the presence of small amounts of salt is greater than in the absence of salt. When the salt concentration reaches a critical limit (when all the exposed ions are saturated by small ions), a maximum in the UCST was observed, corresponding to the thermal energy required in overcoming the strong electrostatic attractive forces. Further increase in the salt concentration (>0.35 wt % NaCl) results in the shielding of intermolecular electrostatic attraction, which facilitates the dissolution of polymer chains. This behavior is commonly referred to as the "antipolyelectrolyte" behavior of polyampholytes. Thus, less thermal energy is required to negate the intermolecular electrostatic attraction in the presence of excess amounts of salt, which is reflected by the reduction in the UCST.

At temperatures beyond the UCST, the polymer exists as an extended coil in dilute aqueous solution instead of the compact structure observed below the UCST. The effect of salt on the hydrodynamic radius of betainized PDMAEMA homopolymer was reported by Armes and co-workers, where the hydrodynamic radius increased with increasing salt concentration, and this phenomenon was explained on the basis of the antipolyelectrolyte effect.[37] We report for the first time the UCST of Bet-PDMAEMA-*b*-C_{60} in aqueous solution as a function of salt concentration (Figure 4). It is evident that, in the presence of

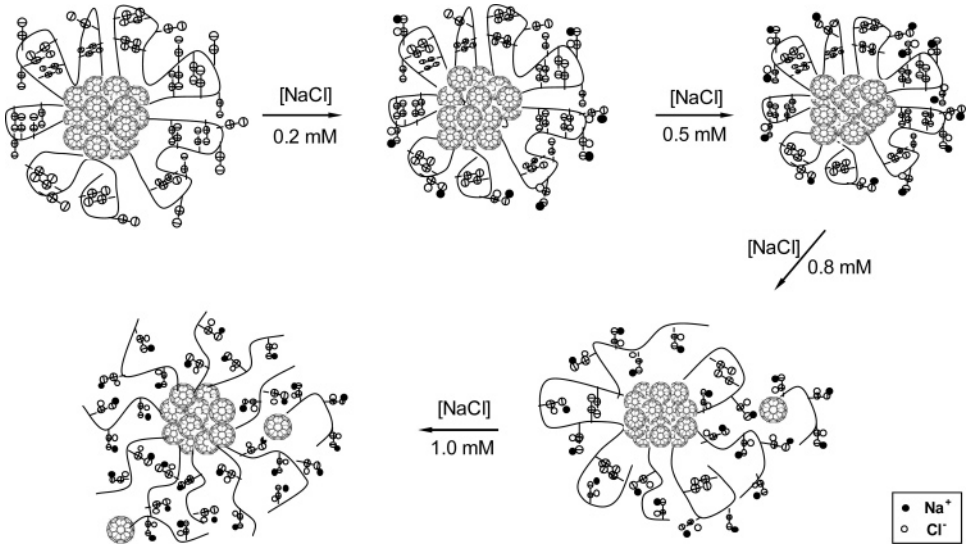

Figure 5. Schematic representation of the aggregation behavior of Bet-PDMAEMA-*b*-C_{60} in the presence of different concentrations of NaCl.

lower concentrations of salt, the betainized polymer exhibits "polyelectrolyte" behavior, where the UCST increases with the addition of NaCl. However, after a critical salt concentration, the betainized polymer displayed antipolyelectrolyte character, where the UCST decreases with increasing NaCl concentration.

Self-Assembly Behavior of Bet-PDMAEMA-*b*-C_{60}. Betainized polymers are soluble only in aqueous salt solution and at temperature greater than the UCST. Since Bet-PDMAEMA-*b*-C_{60} is soluble in 0.5 M NaCl aqueous solution at room temperature, its self-assembly behavior was examined and discussed in this section. Addition of NaCl not only decreases the intermolecular attractive interaction but also shields the electrostatic repulsive interaction between charged segments, imparting enhanced chain flexibility of Bet-PDMAEMA segments. Since laser light scattering is a versatile research tool to study C_{60}-containing amphiphiles,[41] the solution behaviors of both Bet-PDMAEMA and Bet-PDMAEMA-*b*-C_{60} were studied by laser light scattering. Figure 6a,b shows the typical decay time distribution functions of 0.1 wt % Bet-PDMAEMA-*b*-C_{60} and Bet-PDMAEMA solution at different scattering angles. Although Bet-PDMAEMA revealed a monomodal distribution, a bimodal distribution was observed from the decay time distribution of Bet-PDMAEMA-*b*-C_{60}. The dependence of decay rate Γ on q^2 was examined, where q is the scattering vector [$q = 4\pi n \sin(\theta/2)/\lambda$, where n is the refractive index of the solvent, θ is the scattering angle, and λ is the wavelength of the incident laser light in a vacuum], and results are shown in Figure 7. A linear dependence of Γ on q^2 indicates that both decays are related to translational diffusion, suggesting the coexistence of two types of scattering objects in solution. The translational diffusion coefficients D can be determined from the slopes of decay rate Γ and q^2.

DLS measurements were conducted on different polymer concentrations (0.2, 0.4, 0.6, 0.8, 1.0 wt %) in the presence of 0.5 M NaCl to examine the concentration dependence of the diffusion coefficients. It is evident from Figure 8 that both diffusion coefficients are independent of polymer concentration, which indicates that Bet-PDMAEMA-*b*-C_{60} aggregates are produced in solution via the closed association mechanism. By extrapolating the diffusion coefficients to zero concentration, the diffusion coefficients in the infinite dilute solution (D_0) were determined. The hydrodynamic radius of the scattering objects

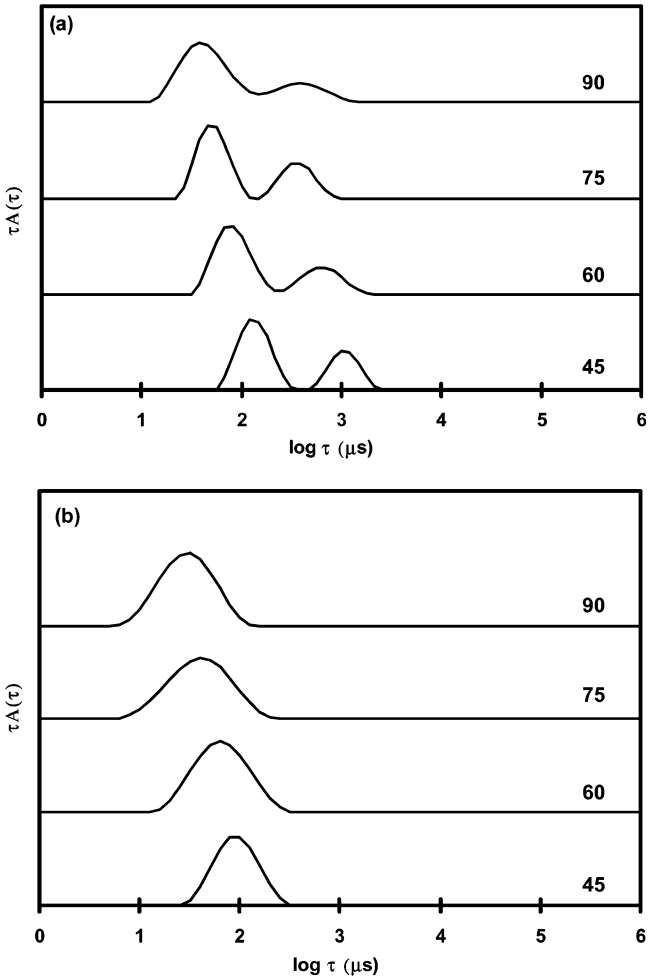

Figure 6. Decay time distribution functions of 0.2 wt % of Bet-PDMAEMA-*b*-C_{60} (a) and Bet-PDMAEMA (b) measured at different scattering angles and at 25 °C.

can be determined using the Stokes−Einstein relationship

$$R_h = \frac{k_B T}{6\pi\eta D_0} \tag{2}$$

where k_B is the Boltzmann constant and η is the solvent viscosity. From the DLS results performed at different scattering

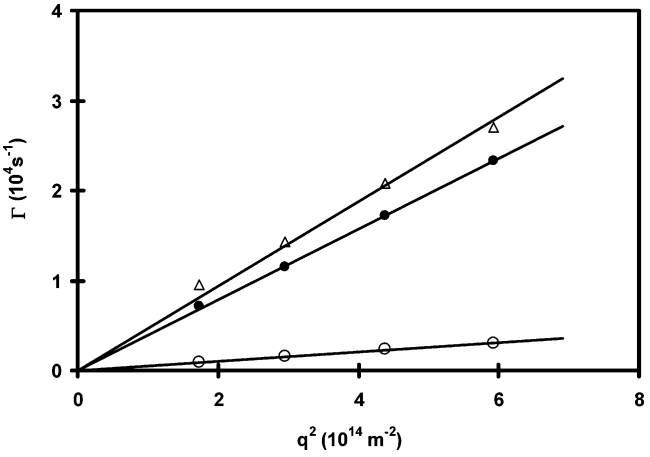

Figure 7. Dependence of the decay rate Γ on the square of the scattering vector (q^2) for 0.2 wt % Bet-PDMAEMA-*b*-C_{60} (filled circles for fast mode and open circles for slow mode) and Bet-PDMAEMA (triangles).

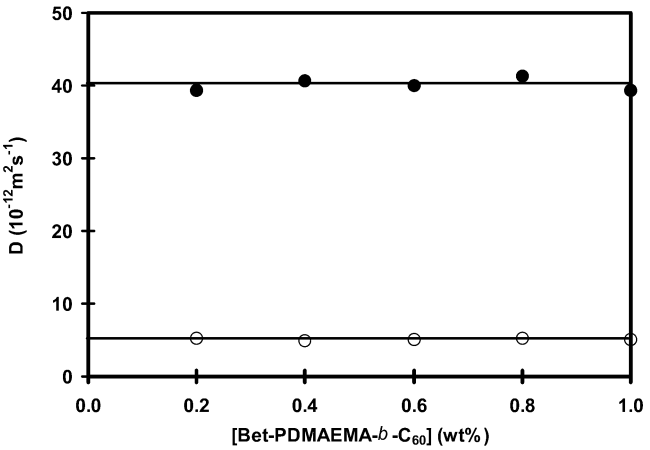

Figure 8. Concentration dependence of Bet-PDMAEMA-*b*-C_{60} translational diffusion coefficients, where the filled circles are the fast decay mode and the open circles are the slow decay mode.

angles and different concentrations, the R_h values of fast and slow modes were found to be ~6 and ~47 nm, respectively. On the basis of the polymer molecular weight and theoretically calculated R_h values, the fast mode is most likely to correspond to unimers, while the R_h of the large particles (slow mode) corresponds to either nonequilibrium aggregates or micelles comprising the hydrophobic C_{60} core and solvated Bet-PDMAEMA corona. However, the 0.1 wt % Bet-PDMAEMA homopolymer in 0.5 M NaCl solution possesses a unimodal distribution in the decay time distribution function. The R_h determined from the decay time distribution function is ~5 nm, which corresponds to Bet-PDMAEMA unimers, in agreement with the fast mode determined for 0.1 wt % Bet-PDMAEMA-*b*-C_{60} solution. This reinforces the observation that hydrophobic C_{60} in Bet-PMAEMA-*b*-C_{60} influences the formation of nonequilibrium aggregates or micelles in solution.

Static light scattering was also performed to further elucidate the aggregation behavior of Bet-PDMAEMA-*b*-C_{60} in 0.5 M NaCl solution. Using SLS, one can determine the *z*-averaged radius of gyration (R_g) and the weight-averaged molecular weight (M_w) of the particles in solution. Due to the strong solvent and solute interaction, a Berry plot was used to determine the weight-averaged molecular weight M_w, A_2, and R_g.

$$\left(\frac{KC}{R_\theta}\right)^{0.5} = \left(\frac{1}{M_w}\right)^{0.5}\left(1 + \frac{1}{6}q^2R_g^{\,2}\right)(1 + A_2M_wC) \qquad (3)$$

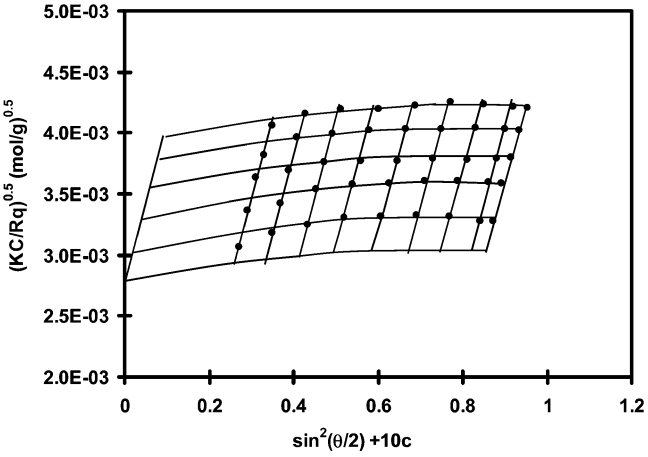

Figure 9. Typical Berry plot of Bet-PDMAEMA-*b*-C_{60} at room temperature in 0.5 M NaCl aqueous solution.

where K ($=4\pi^2n^2(dn/dC)^2/N_A\lambda^4$) is an optical constant, with N_A, n, and λ being Avogadro's number, the solvent refractive index, and the wavelength of the light in a vacuum, respectively. dn/dC is the refractive index increment of the polymer solution obtained from a differential refractometer, C is the polymer concentration, R_θ is the excess Rayleigh ratio, M_w is the weight-averaged molar mass, and R_g is root-mean square *z*-averaged radius of gyration. A_2 is the second viral coefficient, and q is the scattering wave vector. The values of the refractive index increment dn/dC of Bet-PDMAEMA-*b*-C_{60} in the 0.5 M NaCl determined from BI-DNDC differential refractometer were found to be 0.126 g/mL. Figure 9 shows a typical Berry plot for the Bet-PDMAEMA-*b*-C_{60}. The slight curvature in the Berry plot is probably related to the bimodal distribution of unimers and aggregates in solution or associated with the contribution of $P(q)$ and $S(q)$ from the large aggregate in solution. The apparent weight-averaged molecular weight M_w was determined to be $\sim 1.60 \times 10^5$ g/mol. Thus, the averaged aggregation number could be determined by the quotient of the aggregate M_w and the unimer M_w. Since there are two types of particles in solution and the percentage of the unimers can be determined from DLS, it is found that the aggregation number N_{agg} of the aggregates was about 25.[42] At the same time, the *z*-averaged radius of gyration (R_g) was found to be ~42 nm, but it is more sensitive to large particles in solution. From the definition of the radius of gyration, the R_g of large particles can be determined on the basis of the following relationship

$$R_g^{\,2} = \frac{\sum n_iM_i^2(R_g^{\,2})_i}{\sum n_iM_i^2} \qquad (4)$$

The R_g of aggregates was found to be 43.5 nm. Combining with the DLS data, the ratio of R_g/R_h was found to be ~0.93, and this value is probably related to micelles with a more compact structure, which is further supported by the fractal dimension measurement.

Transmission Electron Microscopy. To further elucidate the aggregation behavior of Bet-PDMAEMA-*b*-C_{60}, morphological study was carried out using a transmission electron microscope (TEM). Figure 10 shows the TEM images of Bet-PDMAEMA-*b*-C_{60} polymer above the UCST (~35 °C, in the absence of salt) and in the presence of 0.5 M NaCl solution at room temperature. An abundance of spherical aggregates in the form of clusters was obtained in aqueous solution above the UCST (Figure 10a). Due to the rapid drying process, the changes in the surface tension caused the spherical aggregates to agglomer-

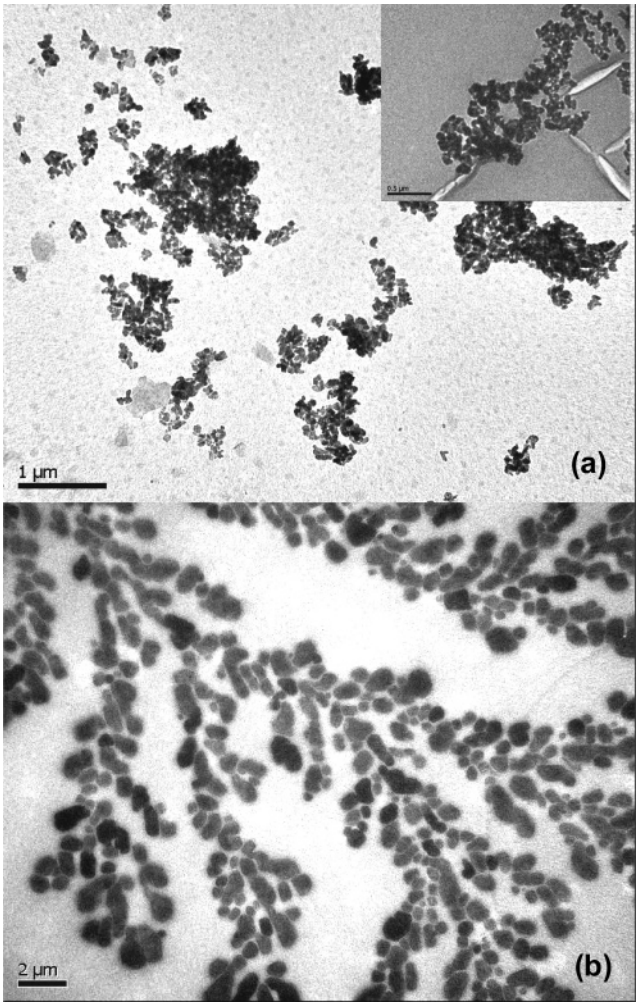

Figure 10. TEM micrographs of 0.2 wt % Bet-PDMAEMA-*b*-C_{60} in aqueous solution (a) in absence of salt (above UCST) and (b) in the presence of 0.5 M NaCl.

ate to form clusters. Since the dehydration process takes place during drying, the radii of small spherical aggregates were found to be ~35 nm, which is smaller than the R_h determined from DLS. In the presence of salt at a temperature below the UCST, the formation of an interesting fractal pattern in the submicron range was observed (Figure 10b). Such controlled fractal morphology was observed for neutralized PMAA-*b*-C_{60} but not for PDMAEMA-*b*-C_{60} in salt solution. The negative charges on the surface of a large compound micelle (LCM) for the PMAA-*b*-C_{60} in salt solution are critical to the fractal growth process,[25] where the LCMs act as nucleating sites for the crystallization of NaCl to produce the controlled fractal pattern. In the case of Bet-PDMAEMA-*b*-C_{60} in salt solution, the sodium ions are condensed on the negatively charged surface ($-SO_3^-$-Na^+) of the micelle, and each micelle acts as a nucleating site that controls the crystallization of NaCl. We also performed TEM on the Bet-PDMAEMA in NaCl solution, and no fractal pattern was observed, instead only NaCl crystals were observed. This further reinforced the importance of the C_{60} core, which acts as a nucleating agent in the production of the fractal structure. The progressive diffusion-controlled growth of sodium chloride crystals during the drying process produces the nanoscale fractal patterns shown in Figure 10b.

Conclusions

A well-defined PDMAEMA-*b*-C_{60} was synthesized using ATRP and betainized with 1,3-sulfobetaine to yield Bet-PDMAEMA-*b*-C_{60}. Blocking of C_{60} to Bet-DMAEMA increases the UCST of the polymer in aqueous media. The presence of salt shifts the UCST of a Bet-PDMAEMA-*b*-C_{60} aqueous solution. At lower salt concentrations, the UCST of the polymer increases with salt concentration due to the binding of small electrolyte on the exposed surface of the ions. At the critical electrolyte concentration, the UCST of the polymer starts to decrease due to the "antipolyelectrolyte" effect. Bet-PDMAEMA-*b*-C_{60} is soluble in 0.5 M NaCl aqueous solution at room temperature; however, they self-assemble to form micelle in aqueous solution with a hydrodynamic radius of ~47 nm, coexisting with a large amount of Bet-PDMAEMA-*b*-C_{60} unimers in solution. The TEM micrograph shows the formation of a controlled fractal pattern in the presence of aqueous salt solution when dried. The utility of such templating and patterning methodology will be further extended to other salt systems and this can potentially be exploited for many biomedical applications.

Acknowledgment. We would like to acknowledge the financial supports provided by the Singapore-MIT Alliance and Ministry of Education, Singapore.

References and Notes

(1) Yen, W.; Jing, T.; Alan, G. M.; James, G. M.; Allan, L. S.; Dayton, J. *Chem. Commun.* **1993**, 603.
(2) Jehoulet, C.; Bard, A. J.; Wudl, F. *J. Am. Chem. Soc*. **1991**, *113*, 5456.
(3) Deguchi, S.; Alargov, R. G.; Tsuji, K. *Langmuir* **2001**, *17*, 6013.
(4) Martin, N.; Sanchez, L.; Liescas, B.; Perez, I. *Chem. Rev.* **1998**, *98*, 2527.
(5) Diederich, F.; Thilgen, C. *Science* **1996**, *271*, 317.
(6) Geckeler, K. E.; Samal, S. *Polym. Int.* **1999**, *48*, 743.
(7) Jin, H.; Chen, W. Q.; Tang, X. W.; Chiang, L. Y.; Yang, C. Y.; Schloss, J. V.; Wu, J. Y. *J. Neurosci. Res*. **2000**, *62*, 600.
(8) Chen, I. W.; Lin, A. T.; Don, D. L.; Kanakamma, P. P.; Shen, C. K. F.; Luh, T. Y.; Hwang, K. C. *J. Med. Chem*. **1999**, *2*, 4614.
(9) Filippone, S.; Heimann, F.; Rassat, A. *Chem. Commun.* **2002**, 1508.
(10) Samal, S.; Geckeler, K. E. *Chem. Commun.* **2000**, 1101.
(11) Konarev, D. V.; Lyubovskaya, R. N. *Russ. Chem. Rev.* **1999**, *68*, 19.
(12) Cerar, J.; Skerjanc, J. *J. Phys. Chem. B* **2003**, *10*, 8255.
(13) Richardson, C. F.; Schuster, D. I.; Wilson, S. R. *Org. Lett*. **2000**, *2*, 1011.
(14) Chiang, L. Y.; Bhonsle, J. B.; Wang, L.; Shu, S. F.; Chang, T. M.; Hwu, J. R. *Tetrahedran* **1996**, *52*, 4963.
(15) Yang, D.; Li, L.; Wang, C. *Mater. Chem. Phys*. **2004**, *87*, 114.
(16) Tan, C. H.; Ravi, P.; Dai, S.; Tam, K. C.; Gan, L. H. *Langmuir* **2004**, *20*, 9882.
(17) Goswami, T. H.; Singh, R.; Alam, S.; Mathur, G. N. *Chem. Mater*. **2004**, *16*, 2442.
(18) Riegel, I. C.; Eisenberg, A. *Langmuir* **2002**, *18*, 3358.
(19) Sitharaman, B.; Asokan, S.; Rusakova, I.; Wong, M. S.; Wilson, L. J. *Nano Lett*. **2004**, *4*, 1759.
(20) Sitharaman, B.; Bolskar, R. D.; Rusakova, I.; Wilson, L. J. *Nano Lett.* **2004**, *4*, 2373.
(21) Wang, X.; Goh, S. H.; Lu, Z. H.; Lee, S. Y. Wu, C. *Macromolecules* **1999**, *32*, 2786.
(22) Yang, J.; Li, L.; Wang, C. *Macromolecules* **2003**, *36*, 6060.
(23) Dai, S.; Ravi, P.; Tan, C. H.; Tam, K. C. *Langmuir* **2004**, *20*, 8569.
(24) Ravi, P.; Dai, S.; Tan, C. H.; Tam, K. C. *Macromolecules* **2005**, *38*, 933.
(25) Tan, C. H.; Ravi, P.; Dai, S.; Tam, K. C. *Langmuir* **2004**, *20*, 9901.
(26) Teoh, S. K.; Ravi, P.; Dai, S.; Tam, K. C. *J. Phys. Chem. B.* **2005**, *109*, 4431.
(27) Ladenheim, H.; Morawetz, H. *J. Polym. Sci.* **1957**, *26*, 251.
(28) Lowe, A. B.; McCormick, C. L. *Chem. Rev.* **2002**, *102*, 4177.
(29) Favresse, P.; Laschewsky, A. *Polymer* **2001**, *42*, 2755.
(30) Kudaibergenov, S. E. *Adv. Polym. Sci.* **1999**, *144*, 115.
(31) Weaver, J. V. M.; Armes, S. P.; Butun, V. *Chem. Commun*. **2002**, 2122.
(32) Arotcarena, M.; Heise, B.; Ishaya, S.; Laschewsky, A. *J. Am. Chem. Soc*. **2002**, *124*, 3787.
(33) Izumrudov, V. A.; Zelikin, A. N.; Zhiryakova, M. V.; Jaeger, W.; Bohrisch, J. *J. Phys. Chem. B* **2003**, *107*, 7982.

(34) Johnson, K. M.; Fevola, M. J.; McCormick, C. L. *J. Appl. Polym. Sci.* **2004**, *92*, 647.
(35) Miyazawa, K.; Winnik, F. M. *Macromolecules* **2002**, *35*, 2440.
(36) Bohrisch, J.; Schimmel, T.; Engelhardt, H.; Jaeger, W. *Macromolecules* **2002**, *35*, 4143.
(37) Lowe, A. B.; Billingham, N. C.; Armes, S. P. *Macromolecules* **1999**, *32*, 2141.
(38) Waziri, S. M.; Abu-Sharkh, B. F.; Ali, S. A. *Biotechnol. Prog.* **2004**, *20*, 526.
(39) Lowe, A. B.; Vamvakaki, M.; Wassall, M. A.; Wong, L.; Billingham, N. C.; Armes, S. P.; Lloyd, A. W. *J. Biomed. Mater. Res.* **2000**, *52*, 88.
(40) Schulz, D. N.; Peiffer, D. G.; Agarwal, P. K.; Larabee, J.; kaladas, J. J.; Soni, L.; Handwerker, B.; Garner, R. T. *Polymer* **1986,** *27*, 1734.
(41) Zhou, S,; Burger, C.; Chu, B.; Sawamura, M.; Nagahama, N.; Toganoh, M.; Hackler, U.; Isobe, H.; Nakamura, E. *Science* **2001**, *291*, 1944.
(42) Dai, S.; Tam, K. C.; Jenkins, R. D. *Macromolecules* **2000**, *33* 404.